Semi- and Fully Interpenetrating Polymer Networks Based on Polyurethane–Polyacrylate Systems. VII. Polyurethane–Poly(methyl Acrylate) Interpenetrating Polymer Networks

D. J. HOURSTON and J. A. McCLUSKEY, *Department of Chemistry, University of Lancaster, Lancaster LA1 4YA, United Kingdom*

Synopsis

A series of polyurethane–poly(methyl acrylate) sequential interpenetrating polymer networks containing 40 wt % polyurethane were prepared. The triol/diol ratio used in the preparation of the first formed polyurethane network was changed so that the average molecular weight between crosslinks ranged from 9500 to 500 g/mol. In addition to decreasing this average molecular weight, changing the triol/diol ratio alters the hard segment content of the polyurethane. The extent of mixing of the components in these IPNs was investigated using electron microscopy, dynamic mechanical analysis, tensile testing, and sonic velocity measurements. The polyurethane networks were also characterized by swelling studies. It was concluded that, as the triol/diol ratio increased, the extent of mixing increased and there was evidence of phase separation of the hard segments of the polyurethane component at high triol/diol ratios.

INTRODUCTION

The synthesis and the subsequent studies of morphology and properties of interpenetrating polymer networks (IPNs) has attracted increasing attention in recent years.[1–3] It can be said that an IPN has been found when a pair of polymeric networks are synthesized in intimate contact with one another. An ideal IPN would be one in which the networks fully interpenetrate to form many physical, but no chemical, crosslinks. Virtually all IPNs show distinct phase separation, and, consequently, the interpenetration is largely restricted to phase boundaries. Thus, in order to optimize interpenetration, it is desirable that the phases be as small as possible.

If one polymer is linear and the other crosslinked, the product is known as a semi-IPN. Earlier papers[4–9] in this series have dealt with such systems.

A number of distinct ways of preparing IPNs have been developed, and these materials are conveniently classified according to method of synthesis. This, and subsequent, papers in the series will be concerned mainly with sequential IPNs.[10] These are materials in which the networks are formed one after the other. Other types include simultaneous IPNs,[11] latex IPNs,[12] and thermoplastic IPNs.[13] For a full review of IPNs, see Ref. 1.

In this paper we report on the morphology and properties of a series of IPNs based on a polyether urethane (PU) and poly(methyl acrylate) (PMA). The PU was synthesized using toluene diisocyanate (TDI), poly(propylene glycol) (PPG) and trimethylol propane (TMP) as the trifunctional cross-

Journal of Applied Polymer Science, Vol. 30, 2157–2169 (1985)
 CCC 0021-8995/85/052157-13$04.00

linking agent. The diol to triol ratio was altered to give a wide range of molecular weights between crosslinks, $\overline{M}_c$. The PMA network was crosslinked with divinyl benzene.

EXPERIMENTAL

The required amounts of the carefully dried PU precursors, TDI (B.D.H. Chemicals), PPG (Aldrich), and TMP (Aldrich) were dissolved in 60% by weight of destabilized and dried methyl acrylate (B.D.H. Chemicals). The PPG has an $\overline{M}_n$ of 1025 g/mol and an $\overline{M}_w/\overline{M}_n$ of 1.1. The former value was determined by vapor pressure osmometry, and the latter by gel permeation chromatography. The methyl acrylate (MA) contained 0.2 wt % AZBN (Aldrich) to initiate the vinyl polymerisation and 5 wt % divinyl benzene (Cambrian Chemicals) to serve as crosslinker. The mixture was thoroughly blended. Di-*n*-butyl tin dilaurate (B.D.H. Chemicals) was then added (2% w/w of PU) to promote polyurethane formation. The mixture was carefully degassed and then poured into a metal mold.[4] The polyurethane formation was allowed to proceed at room temperature for 24 h. The mold was then heated to 65°C for 18 h and then to 90°C for a further 6 h to polymerize the MA. The resulting sheets were placed in a vacuum oven (30°C) for at least 1 week to remove residual monomer. The weight loss during this period was always less than 3%.

To synthesize the PU sheets, the same procedure was adopted, but the PU precursors were dissolved in inhibited MA which was allowed to evaporate from the PU sheet once the latter had formed. The final stages of this process occurred in a vacuum oven.

To determine the solubility parameters δ_p for the PU networks, pieces of sheet approximately 1 cm^2 were swollen in a series of liquids whose solubility parameter δ_s covered a wide range. Maximum swelling[4] occurred in chloroform which has a δ_s value of 18.8×10^3 (J/m^3)$^{1/2}$. Maximum swelling occurs when the solubility parameter of the material and that of the swelling liquid match.[14]

The polymer–solvent interaction parameter χ was determined using the Bristow and Watson[15] semiempirical equation:

$$\chi = \beta + (V_s/RT)(\delta_s - \delta_p)^2 \tag{1}$$

β is the lattice constant, usually about 0.34, V_s is the molar volume of the swelling agent, and R and T have their usual significance. $\overline{M}_c$ was calculated from the Flory–Rehner[16–18] equation:

$$\nu_e = -\frac{1}{V_s}\left[\frac{\ln(1 - \nu_r) + \nu_r + \chi\nu_r^2}{\nu_r^{1/3} - 2\,\nu_r/F}\right] \tag{2}$$

ν_e is the number of polymer chains per unit volume, F is the functionality of the crosslinking system, which in this case is 3, and ν_r is the equilibrium volume fraction of polymer in the swollen gel. ν_e and $\overline{M}_c$ are related by the polymer density l:

$$\nu_e = l/\overline{M}_c \tag{3}$$

As the polyurethane networks were crosslinked in the swollen state, the influence this had on $\overline{M}_c$ was taken into account by the use of the Tobolsky front factor,[19,20] which can be replaced by $\phi_r^{2/3}$. ϕ_r is the volume fraction of rubber present at the time of crosslinking. Thus, eq. (3) is modified as follows:

$$\nu_e = (l/\overline{M}_c)\phi_r^{2/3} \tag{4}$$

Transmission electron micrographs were obtained using a Hitachi electron microscope (Model HU-11B). The samples were first stained using osmium tetroxide vapor. The stress–strain measurements (20°C) were made with a Howden tensometer at a strain rate of 2.5 cm/min. Standard dumbbell specimens were used, and strain was defined as change in length divided by original length.

V_L, the longitudinal sonic velocity, was measured (20°C) with a Morgan pulse propagation meter (PPM-5R).[21] The dynamic mechanical data were obtained with a Rheovibron dynamic mechanical viscoelastometer (Model DDV-II-B) at a heating rate of approximately 1°C/min.

RESULTS AND DISCUSSION

The PU Networks

A number of studies of the properties and morphology of segmented PU elastomers have been reported.[22–26] Morphological studies[27–29] have shown that the two kinds of chain segments in segmented PUs can separate in some instances into microphases. The mechanical properties of polyurethane elastomers are essentially a consequence of a combination of segment flexibility, degree of crosslinking, chain entanglement, rigidity of aromatic units, hydrogen bonding, and other interactions. As these interactions are temperature-dependent, mechanical properties of segmented PUs deteriorate with increasing temperature. This can be overcome by the introduction of permanent crosslinks.[30] Even with crosslinking,[30] microphase segregation of hard and soft segments generally occurs, the hard segments sometimes forming crystalline domains. Crystallinity and crosslinking are important variables in determining mechanical behavior.

Dearlove and Campbell[31] investigated the effects of catalyst and triol/diol ratio on polyurethane network formation and found these factors to be important. Similar studies have been reported by Allen et al.[32] and Zia.[33]

The triol/diol ratios and $\overline{M}_c$ values of the PU networks investigated are shown in Table I. Figure 1 shows the stress–strain behavior of the PU networks. As expected, for an increase in crosslink density there is a reduction in elongation at break, E_B, accompanied by an increase in tensile strength. Table II summarises the essential data. PU1, PU2, and PU3 show typical rubbery behavior. PU4 is the toughest having a comparatively large stress at break, but reduced elongation. PU5 behaves as a fairly glassy polymer, showing a low E_B value, but quite a high tensile strength.

TABLE I
PU Network Data

Code	Triol/diol[a]	$\overline{M}_c$ (g/mol)
PU 1	0.375	9,500
PU 2	0.50	3,300
PU 3	0.625	2,000
PU 4	0.75	1,200
PU 5	0.875	500

[a] mole fraction

With these networks, two effects are influencing properties. There is a considerable change in crosslink density, but there is also a significant change in the molecular structure of the PU networks as the concentration of relatively inflexible TDI residues rises as the triol/diol ratio increases. Thus, the two extremes range from a material formed from fairly flexible chains to one containing a much higher concentration of rigid in-chain phenyl groups.

Rubbery materials have low longitudinal sonic velocities relative to plastics. The V_L values of the five PU networks are shown in Figure 2. It is apparent that samples PU1 to PU3 show values typical[34] of soft rubbery materials having V_L values below 0.5 km/s and show a linear increase in V_L as the triol/diol ratio is changed. With PU4, there is a significant increase in V_L, followed in PU5 by an even greater rise, resulting in a marked curvature of the V_L–triol/diol ratio plot at high levels of crosslinking and in V_L values typical[34] of glassy polymers. Again, these observations are a consequence both of the change in modulus arising from increased crosslinking and of the increasing hard segment content leading to stiffer molecules.

The tan δ–temperature plots are shown in Figure 3. Table III summarises the essential data. The apparent activation energies E_A for the glass transitions were determined from equation 5.

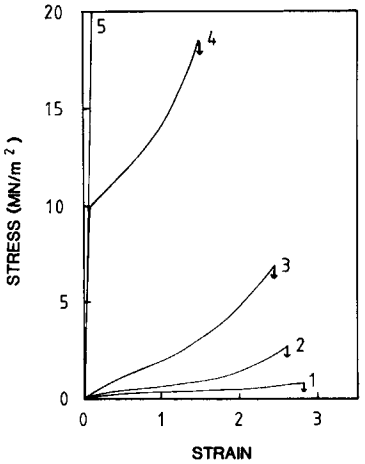

Fig. 1. Stress–strain curves (20°C) for PU1 (1), PU2 (2), PU3 (3), PU4 (4), and PU5 (5).

TABLE II
Stress–Strain Data (20°C) for the PU Networks

Code	Tensile strength (MN/m^2)	100% modulus (MN/m^2)	Elongation at break (%)
PU 1	0.8	0.3	280
PU 2	2.6	0.6	265
PU 3	6.8	1.8	245
PU 4	18.5	14.0	150
PU 5	26.5	—	12.5

$$\ln \frac{\omega_1}{\omega_2} = \frac{E_A}{R}\left(\frac{1}{T_2} - \frac{1}{T_1}\right) \tag{5}$$

ω_1 and ω_2 are the applied frequencies and T_1 and T_2 are the corresponding temperatures at which the maximum value of tan δ occurs. PU1 has a maximum tan δ value, tan δ_{max}, of 0.97 at −3°C. The high temperature side of the curve shows a broadening typical of segmented PUs. Consequently, the half-peak width extends over a 45°C temperature range. For PU2, the position of tan δ_{max} is shifted by 18° and its magnitude is reduced. There is also a broadening of the peak. A similar shift and peak broadening is observed for PU3. These effects are typical of an increasing level of cross-linking in a polymer network.[35] The transition seen for the first three networks is believed to be essentially the soft segment glass transition. However, the accompanying copolymer effect must be remembered. PU4 shows a very broad relaxation and a peak shift relative to PU3 of 78°C. There is a slight inflection in the tan δ–temperature plot at around 60°C indicating the possibility of two mechanisms. For PU5, a distinct shoulder occurs on the low temperature side of the main transition, clearly indicating a dual mechanism. The upper transition is likely to be associated with hard segment domains. North and Reid[26] have reported a T_g of 109°C for a linear

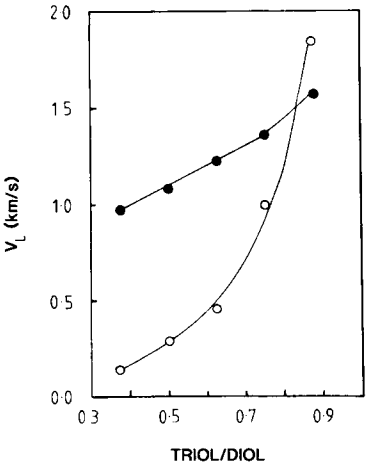

Fig. 2. V_L-triol/diol ratio for the PU networks (○) and the IPNs (●).

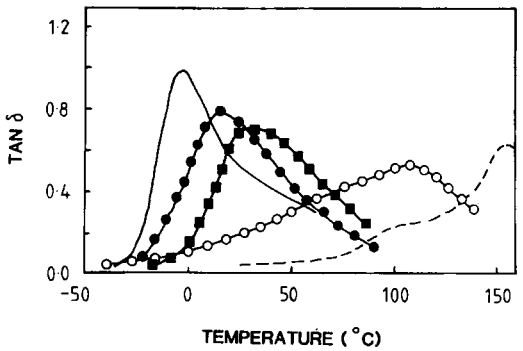

Fig. 3. Tan δ–temperature plots (35 Hz) for PU1 (—), PU2 (●), PU3 (■), PU4 (○), and PU5 (- - -).

polyurethane prepared from butane-1,4-diol and methylene bis(phenyl isocyanate). It is reasonable to suppose that hard segments in a crosslinked system synthesized from TDI and TMP would have a higher T_g.

Sample 5 showed signs of degradation at temperatures above 165°C.

The E_A values for PU1, PU2, and PU4 are, within experimental error, the same. However, PU3 has a significantly higher value. A speculative interpretation is that, for the PU3 composition, phase separation of the hard and soft blocks is developing and influencing soft segment motions. These motions may be less restricted in PU4 where phase separation is more complete.

Figures 4 and 5 show the dynamic storage modulus E' and the dynamic loss modulus E'' vs. temperature plots. From the E'–temperature data, PU1, PU2, and PU3 show a single transition, but PU4 shows evidence of a second mechanism. From the E''–temperature curves (Fig. 5), the shifting and broadening of the glass transition is very evident for the three highest $\overline{M}_c$ samples. For PU4, two mechanisms can be decerned with the more prominent one occuring at a temperature below that shown by network PU3. If this lower transition is taken to be the soft segment glass transition, it follows for PU3 that some other factor is influencing the ability of the soft segments to move. This accords with the observed apparent activation energies in Table III.

The PU–PMA IPNs

Sperling et al.[2,36] have reported that the level of crosslinking in the first formed network of a sequential IPN significantly influences its morphology

TABLE III
Dynamic Mechanical Data (35 Hz) for the PU Networks

Code	T_g (°C)	Tan δ_{max}	Half peak width (°C)	E_A (kJ/mol)
PU 1	−3	0.97	45	120
PU 2	15	0.79	56	123
PU 3	30	0.70	61	162
PU 4	108	0.52	>100	124
PU 5	156	0.64	—	—

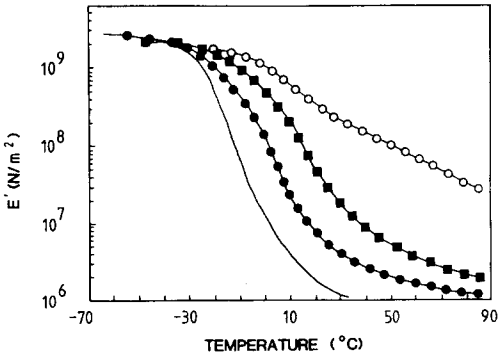

Fig. 4. E'–temperature plots (35 Hz) for PU1 (—), PU2 (●), PU3 (■), and PU4 (○).

and properties. This effect is further investigated in this study. The composition of all the IPNs was constant at 40 PU–60 PMA (w/w), and the PU networks of these five IPNs are identical to those just discussed. Hourston and Zia[5] have shown that there is significant dual phase continuity for a compositionally identical semi-1-IPN. The full IPN should exhibit enhanced continuity of the components.

Figures 6–8 are transmission electron micrographs of the IPNs in which the $\overline{M}_c$'s of the PU component are nominally 2000 (IPN 3), 1200 (IPN 4), and 500 (IPN 5) g/mol, respectively. The dark areas in the micrographs are PU-rich regions, as it is known[37] that OsO_4 preferentially stains the PU component. Close examination of enlargements of these micrographs shows that all the IPNs have a cell-like[38] structure. As the PU $\overline{M}_c$ value decreases, the size of the PU-rich regions also decrease significantly. Increasing the level of crosslinking of the first formed network[2,36] leads to a finer morphology.

Figure 9 shows the stress-strain curves of the IPNs. Increasing the triol content of the PU network clearly influences the stress-strain response. As the PU network $\overline{M}_c$ decreases, E_B also decreases, but the tensile strength increases. Table IV summarises the data. Comparing the IPNs with the corresponding PU networks (Table II), it is apparent that IPN 1 and IPN 2 show markedly improved tensile strength and 100% modulus, but have fairly similar E_B values. IPN 3 has a marginally superior tensile strength.

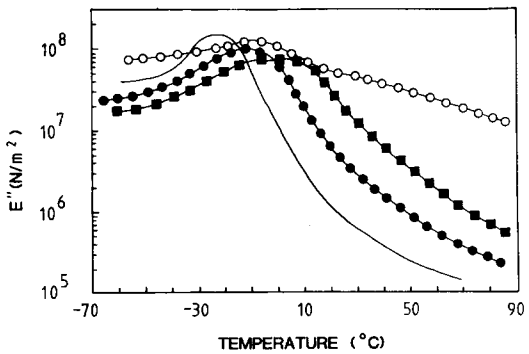

Fig. 5. E''–temperature plots (35 Hz) for PU1 (—), PU2 (●), PU3 (■), and PU4 (○).

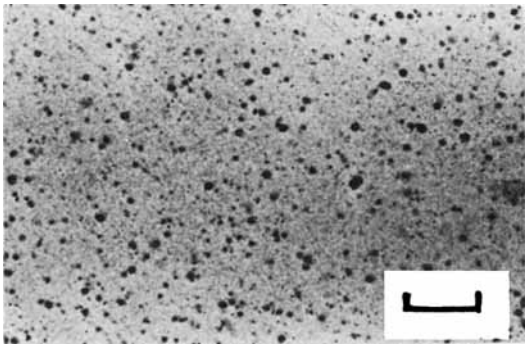

Fig. 6. Transmission electron micrograph of IPN3. Bar = 500 nm.

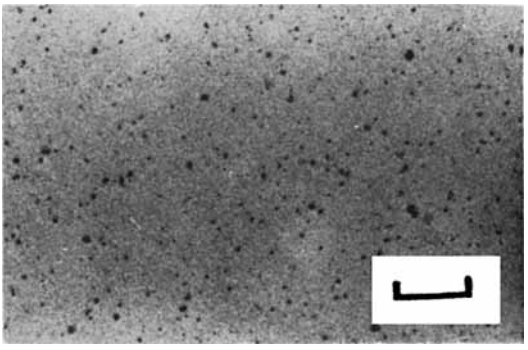

Fig. 7. Transmission electron micrograph of IPN4. Bar = 500 nm.

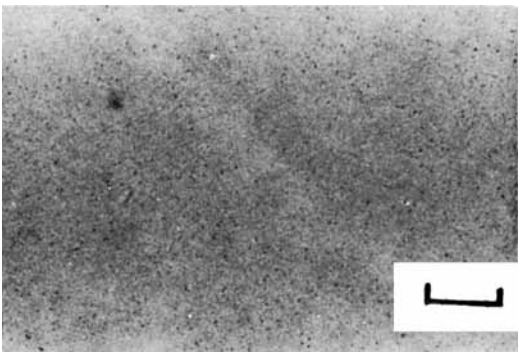

Fig. 8. Transmission electron micrograph of IPN5. Bar = 500 nm.

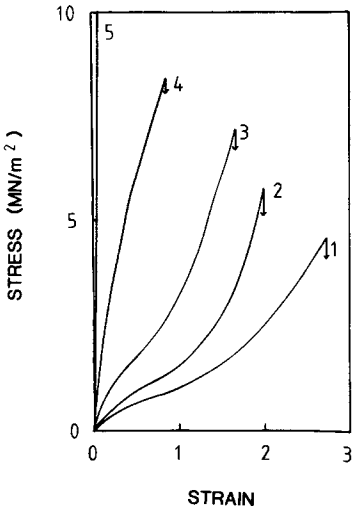

Fig. 9. Stress–strain curves (20°C) for IPN1 (1), IPN2 (2), IPN3 (3), IPN4 (4), and IPN5 (5).

IPN 4 and IPN 5 have tensile strengths which are inferior to the corresponding PU networks.

When tested under identical conditions, it was found[39] that a PMA network crosslinked with 5 wt % divinyl benzene had a tensile strength of 13 MN/m², a 100% modulus of 2.7 MN/m² and an elongation at break of 276%. Thus, the transition between IPN 3 and IPN 4 from a situation where the IPN properties were superior to those of the PU networks to the reverse situation will largely be caused by the fact that it is in this region that the above properties of the PMA network become inferior to those of the PU 4 and PU 5 networks.

The dynamic mechanical data for this series of samples are complex to interpret. It is helpful to consider the IPNs in two groups. The first being materials (IPN 1–IPN 3) where the PU T_g is less than that of the PMA network and the second is the converse situation. The data are shown in Figures 10–12, and some of the more salient points are presented in Table V. When comparing data in Table V with that in Table III, note that the experimental frequencies are slightly different. From the known apparent activation energies of the networks, it can be calculated that this difference

TABLE IV
Stress–Strain Data (20°C) for the IPNs

Code	$\bar{M}_c$ (PU network) (g/mol)	Tensile strength (MN/m²)	100 % modulus (MN/m²)	Elongation at break (%)
IPN 1	9500	4.6	0.95	275
IPN 2	3300	5.8	1.55	195
IPN 3	2000	7.2	3.30	165
IPN 4	1200	8.35	—	80
IPN 5	500	14.0	—	20

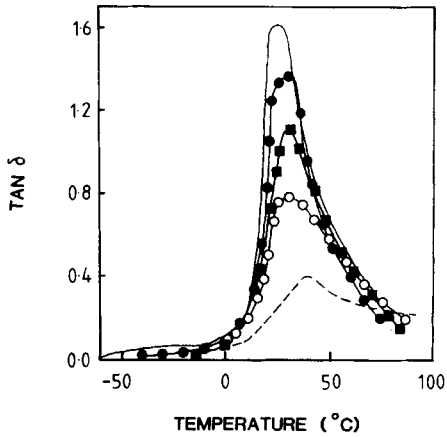

Fig. 10. Tan δ–temperature plots (11 Hz) for IPN1 (—), IPN2 (●), IPN3 (■), IPN4 (○), and IPN5 (- - -).

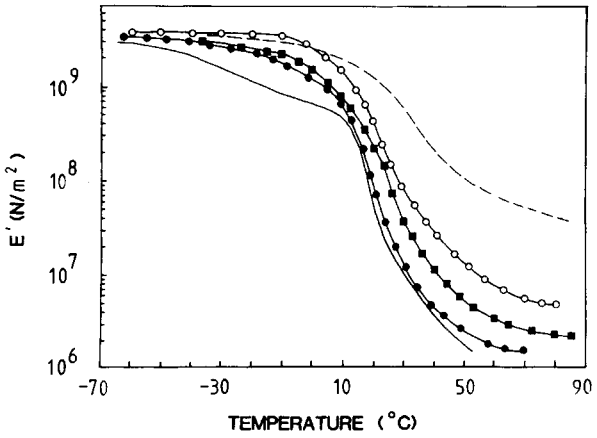

Fig. 11. *E'*–temperature plots (11 Hz) for IPN1 (—), IPN2 (●), IPN3 (■), IPN4 (○), and IPN5 (- - -).

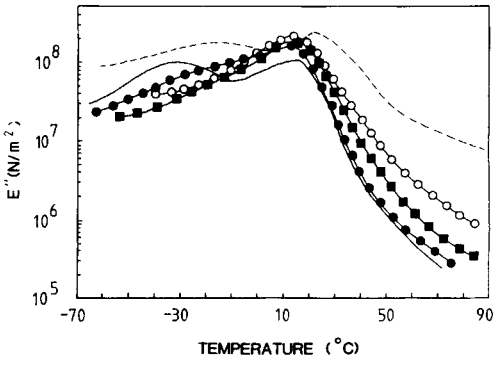

Fig. 12. *E''*–temperature plots (11 Hz) for IPN1 (—), IPN2 (●), IPN3 (■), IPN4 (○), and IPN5 (- - -).

TABLE V
Dynamic Mechanical Data (11 Hz) for the IPNs

Code	T_g (°C)	Half peak width (°C)
IPN 1	26	28
IPN 2	29	29
IPN 3	31	36
IPN 4	34	42
IPN 5	39	80

in frequency raises the PU network T_g's by about 3°C. In considering the dynamic mechanical results, it is necessary to know that the PMA network prepared using 5% DVB had an $\overline{M}_c$ of 3,800 g/mol and the T_g occurred at 41°C (11 Hz). It is possible that decreasing $\overline{M}_c$ of network 1 could reduce the efficiency of crosslinking of network 2. If only 1% DVB is used to prepare the homonetwork, the T_g occurs at 32°C (11 Hz). It is assumed, however, in the following discussion that the T_g of the PMA component is always close to 41°C.

From Figure 10 and Table V, it is clear that all five IPNs show one major transition in the tan δ–temperature plots which shifts by only 13°C over the range of crosslinking investigated. For the two IPNs with the highest $\overline{M}_c$ values, a second transition is just discernible. However, in Figures 11 and 12 these lower temperature transitions are more clearly resolved. It is commonly observed in sequential IPNs which exhibit phase separation[6,39] that the transition of the first synthesized network is suppressed. As this network is continuous, even when present at low levels, the suppression is attributed to the fact that many network 1 segments are in close juxtaposition with the yet glassy second component and can only fully relax when the latter reaches its glass transition temperature.

For IPN 1 the glass transition occurs in the tan δ–temperature plot at 26°C, but it is clear from Figures 11 and 12 that there are two transitions to be considered. The lower transition (Fig. 12) is reasonably close to the transition shown by PU1 (Fig. 5) which corresponds to the soft segment glass transition of the homonetwork. Its existence in IPN 1 implies that this material has PU phases. The transition at 26°C probably arises from mixed PU–PMA phases. For IPN 1, the homonetwork T_g's differ by 47°C. Despite the partial overlap of the network tan δ–temperature dispersions, such a separation in dynamic mechanical analysis would lead to the resolution of two transitions if there was a significant amount of PMA present in separated phases. The absence of such a transition, therefore, is taken to indicate that there is substantial enforced mixing in IPN 1.

IPN 2, like IPN 1, shows two transitions in the E'– and E''–temperature plots which are shifted to higher temperatures, indicating an increased level of component mixing. For this IPN, the T_g difference of the networks is reduced to 29°C, but still not too close to prohibit the detection of a significant amount of pure PMA.

With IPN 3, the difference between the T_g's of the component networks is only 14°C with the tan δ–temperature curves overlapping very substan-

tially. Even if the material were substantially phase-separated, the dynamic mechanical technique would probably not be sensitive enough to detect it. However, as the evidence supports increased mixing for IPN 2 over IPN 1, it follows that the trend continues for IPN 3.

It was postulated earlier that phase separation of the hard segments was occurring increasingly for PU 4 and PU 5. For both these PU networks the T_g (tan δ maximum value) was vastly greater than that of the PMA component. IPN 4 shows only one transition at 34°C, but IPN 5, like IPN 1, has (Fig. 12) two transitions. An explanation is that in IPN 5 the PU component is itself phase-separated and the lower transition corresponds to the soft segment T_g raised to higher temperatures by forced mixing with the PMA network.

These dynamic mechanical studies, including the half peak widths in Table V, indicate an increased level of mixing as the triol/diol ratio increases.

Figure 2 shows the V_L–composition plot for the IPNs. This is initially linear, but this linearity ceases at high levels of crosslinking. The V_L value of the PMA homonetwork was found to be 2.2 km/s. The observed V_L values for the IPNs are lower than the algebraic sum of the homonetwork values.

J. A. McCluskey wishes to thank the SERC for a CASE award and Mr. P. Howgate of RAPRA for his help during the work.

REFERENCES

1. L. H. Sperling, *Interpenetrating Polymer Networks and Related Materials*, Plenum, New York, 1981.
2. D. A. Thomas and L. H. Sperling, *Polymer Blends*, D. R. Paul and S. Newman, Eds., Academic, New York, 1978, Vol. 2.
3. H. L. Frisch, K. C. Frisch, and D. Klempner, *Pure Appl. Chem.*, **53**, 1557 (1981).
4. D. J. Hourston and Y. Zia, *J. Appl. Polym. Sci.*, **28**, 2139 (1983).
5. D. J. Hourston and Y. Zia, *J. Appl. Polym. Sci.*, **28**, 3745 (1983).
6. D. J. Hourston and Y. Zia, *J. Appl. Polym. Sci.*, **28**, 3849 (1983).
7. D. J. Hourston and Y. Zia, *J. Appl. Polym. Sci.*, **29**, 629 (1984).
8. D. J. Hourston and Y. Zia, *J. Appl. Polym. Sci.*, **29**, 2951 (1984).
9. D. J. Hourston and Y. Zia, *J. Appl. Polym. Sci.*, **29**, 2963 (1984).
10. L. H. Sperling and D. W. Friedman, *J. Polym. Sci.*, **7**, 425 (1969).
11. L. H. Sperling and R. R. Arnts, *J. Appl. Polym. Sci.*, **15**, 2317 (1971).
12. L. H. Sperling, T. W. Chui, C. Hartman, and D. A. Thomas, *Int. J. Polym. Sci.*, **1**, 331 (1972).
13. D. L. Siegfried, D. A. Thomas, and L. H. Sperling, *J. Appl. Polym. Sci.*, **26**, 177 (1981).
14. G. Gee, G. Allen, and G. Wilson, *Polymer*, **1**, 456 (1960).
15. G. M. Bristow and W. F. Watson, *Trans. Faraday Soc.*, **54**, 1731 (1958).
16. P. J. Flory and J. Rehner, *J. Chem. Phys.*, **11**, 521 (1943).
17. J. P. Bell, *J. Polym. Sci., A-2*, **8**, 417 (1970).
18. G. Krause, *Rubber World*, **135**, 67 (1956).
19. A. V. Tobolsky, D. W. Carlson, and N. Indicator, *J. Polym. Sci.*, **54**, 175 (1961).
20. C. Price, G. Allen, F. De Candia, M. C. Kirkham, and A. Subramanian, *Polymer*, **11**, 486 (1970).
21. A Beamish, R. A. Goldberg, and D. J. Hourston, *Polymer*, **18**, 49 (1977).
22. S. L. Cooper and A. V. Tobolsky, *J. Appl. Polym. Sci.*, **11**, 1361 (1967).
23. S. B. Clough and N. S. Schneider, *J. Macromol. Sci.*, **32**, 553 (1968).
24. T. Kajiyama and W. J. McKnight, *Macromolecules*, **2**, 254 (1969).
25. J. Ferguson, D. J. Hourston, R. Meredith, and D. Patsavoudis, *Eur. Polym. J.*, **8**, 369 (1972).

26. A. M. North and J. C. Reid, *Eur. Polym. J.*, **8**, 1129 (1972).
27. G. M. Estes, S. L. Cooper, and A. V. Tobolsky, *J. Macromol Sci. Rev., Macromol. Chem.*, **C4**, 313 (1970).
28. S. L. Samuels and G. L. Wilkes, *J. Polym. Sci.*, **43**, 149 (1973).
29. C. S. Schollenberger and K. Dinsberg, *J. Elastoplast.*, **5**, 222 (1973).
30. R. R. Lagasse, *J. Appl. Polym. Sci.*, **21**, 2489 (1977).
31. T. J. Dearlove and G. A. Campbell, *J. Appl. Polym. Sci.*, **21**, 1499 (1977).
32. G. Allen, M. J. Bowden, D. J. Blundell, F. G. Hutchinson, G. M. Jeffs, and J. Vyvoda, *Polymer*, **14**, 597 (1973).
33. Y. Zia, Ph.D. thesis, University of Lancaster, 1978.
34. D. J. Hourston and I. D. Hughes, *J. Appl. Polym. Sci.*, **21**, 3093 (1977).
35. L. E. Nielsen, *Mechanical Properties of Polymers*, Reinhold, New York, 1962.
36. A. A. Donatelli, D. A. Thomas, and L. H. Sperling, *Recent Advances in Polymer Blends, Grafts and Block Copolymers*, L. H. Sperling, Ed., Plenum, New York, 1974.
37. S. C. Kim, D. Klempner, K. C. Frisch, W. Radigan, and H. L. Frisch, *Macromolecules*, **9**, 258 (1976).
38. A. J. Curtius, M. J. Covitch, D. A. Thomas, and L. H. Sperling, *Polym. Eng. Sci.*, **12**, 101 (1972).
39. J. A. McCluskey, Ph.D. thesis, University of Lancaster, 1980.

Received July 22, 1984
Accepted September 27, 1984